

# Simultaneous determination of the kinetics of cardiac output, systemic O<sub>2</sub> delivery, and lung O<sub>2</sub> uptake at exercise onset in men

Frédéric Lador, Marcel Azabji Kenfack, Christian Moia, Michela Cautero, Denis R. Morel, Carlo Capelli and Guido Ferretti

*Am J Physiol Regul Integr Comp Physiol* 290:1071-1079, 2006. First published Oct 20, 2005;  
doi:10.1152/ajpregu.00366.2005

## You might find this additional information useful...

---

This article cites 56 articles, 38 of which you can access free at:

<http://ajpregu.physiology.org/cgi/content/full/290/4/R1071#BIBL>

Updated information and services including high-resolution figures, can be found at:

<http://ajpregu.physiology.org/cgi/content/full/290/4/R1071>

Additional material and information about *American Journal of Physiology - Regulatory, Integrative and Comparative Physiology* can be found at:

<http://www.the-aps.org/publications/ajpregu>

---

This information is current as of March 15, 2006 .

*The American Journal of Physiology - Regulatory, Integrative and Comparative Physiology* publishes original investigations that illuminate normal or abnormal regulation and integration of physiological mechanisms at all levels of biological organization, ranging from molecules to humans, including clinical investigations. It is published 12 times a year (monthly) by the American Physiological Society, 9650 Rockville Pike, Bethesda MD 20814-3991. Copyright © 2005 by the American Physiological Society. ISSN: 0363-6119, ESN: 1522-1490. Visit our website at <http://www.the-aps.org/>.

## Simultaneous determination of the kinetics of cardiac output, systemic O<sub>2</sub> delivery, and lung O<sub>2</sub> uptake at exercise onset in men

Frédéric Lador,<sup>1</sup> Marcel Azabji Kenfack,<sup>1</sup> Christian Moia,<sup>1</sup> Michela Cautero,<sup>3</sup> Denis R. Morel,<sup>2</sup> Carlo Capelli,<sup>3</sup> and Guido Ferretti<sup>1,4</sup>

<sup>1</sup>Département de Physiologie, Centre Médical Universitaire, Genève, Switzerland; <sup>2</sup>Département d'Anesthésiologie, Pharmacologie et Soins Intensifs Chirurgicaux, Hôpital Cantonal Universitaire, Bâtiment Opéra, Genève, Switzerland;

<sup>3</sup>Laboratorio di Fisiologia, Dipartimento di Scienze e Tecnologia Biomediche, Università di Udine, Udine, Italy; and

<sup>4</sup>Sezione di Fisiologia Umana, Dipartimento di Scienze Biomediche e Biotecnologie, Università di Brescia, Brescia, Italy

Submitted 24 May 2005; accepted in final form 8 October 2005

**Lador, Frédéric, Marcel Azabji Kenfack, Christian Moia, Michela Cautero, Denis R. Morel, Carlo Capelli, and Guido Ferretti.** Simultaneous determination of the kinetics of cardiac output, systemic O<sub>2</sub> delivery, and lung O<sub>2</sub> uptake at exercise onset in men. *Am J Physiol Regul Integr Comp Physiol* 290: R1071–R1079, 2006. First published October 20, 2005; doi:10.1152/ajpregu.00366.2005.—We tested whether the kinetics of systemic O<sub>2</sub> delivery ( $\dot{Q}aO_2$ ) at exercise start was faster than that of lung O<sub>2</sub> uptake ( $\dot{V}O_2$ ), being dictated by that of cardiac output ( $\dot{Q}$ ), and whether changes in  $\dot{Q}$  would explain the postulated rapid phase of the  $\dot{V}O_2$  increase. Simultaneous determinations of beat-by-beat (BBB)  $\dot{Q}$  and  $\dot{Q}aO_2$ , and breath-by-breath  $\dot{V}O_2$  at the onset of constant load exercises at 50 and 100 W were obtained on six men (age  $24.2 \pm 3.2$  years, maximal aerobic power  $333 \pm 61$  W).  $\dot{V}O_2$  was determined using Grønlund's algorithm.  $\dot{Q}$  was computed from BBB stroke volume ( $Q_{st}$ , from arterial pulse pressure profiles) and heart rate ( $f_{hr}$ , electrocardiography) and calibrated against a steady-state method. This, along with the time course of hemoglobin concentration and arterial O<sub>2</sub> saturation (infrared oximetry) allowed computation of BBB  $\dot{Q}aO_2$ . The  $\dot{Q}$ ,  $\dot{Q}aO_2$  and  $\dot{V}O_2$  kinetics were analyzed with single and double exponential models.  $f_{hr}$ ,  $Q_{st}$ ,  $\dot{Q}$ , and  $\dot{V}O_2$  increased upon exercise onset to reach a new steady state. The kinetics of  $\dot{Q}aO_2$  had the same time constants as that of  $\dot{Q}$ . The latter was twofold faster than that of  $\dot{V}O_2$ . The  $\dot{V}O_2$  kinetics were faster than previously reported for muscle phosphocreatine decrease. Within a two-phase model, because of the Fick equation, the amplitude of phase I  $\dot{Q}$  changes fully explained the phase I of  $\dot{V}O_2$  increase. We suggest that in unsteady states, lung  $\dot{V}O_2$  is dissociated from muscle O<sub>2</sub> consumption. The two components of  $\dot{Q}$  and  $\dot{Q}aO_2$  kinetics may reflect vagal withdrawal and sympathetic activation.

cardiovascular response

AT THE ONSET OF SQUARE-WAVE light aerobic exercise, O<sub>2</sub> consumption increases to attain a steady level, proportional to the exerted mechanical power. Its increase rises at a finite rate in response to the step increase in power, so that an O<sub>2</sub> deficit is incurred in the first minutes of exercise. The O<sub>2</sub> deficit reflects the decrease in high-energy phosphate concentration that is necessary to accelerate aerobic metabolic pathways (5, 19, 35, 37). Analogous to the charge of a single capacitance, the increase in O<sub>2</sub> consumption was described by monoexponential equations (5, 15, 19). The monoexponential decrease in phosphocreatine concentration upon square-wave exercise onset (6, 46) is perhaps the strongest evidence provided so far in favor of this single capacitance model for O<sub>2</sub> consumption. Assum-

ing close correspondence between O<sub>2</sub> consumption by the working muscles and O<sub>2</sub> uptake at the lungs ( $\dot{V}O_2$ ), the  $\dot{V}O_2$  was investigated to gain information on O<sub>2</sub> consumption (15, 16).

This correspondence, however, was questioned. In fact, the kinetics of O<sub>2</sub> consumption requires that it be sustained by adequate O<sub>2</sub> transfer from ambient air to mitochondria. Thus, concomitant with the increase in O<sub>2</sub> consumption, there must be 1) an increase in  $\dot{V}O_2$ ; 2) an increase in O<sub>2</sub> flow in arterial blood [or systemic O<sub>2</sub> delivery ( $\dot{Q}aO_2$ ) that is the product of cardiac output ( $\dot{Q}$ ), times arterial O<sub>2</sub> concentration,  $CaO_2$ ], most of which, during exercise, is directed to the contracting muscles; and 3) an increase in the diffusive O<sub>2</sub> flow from capillaries to mitochondria. Concerning  $\dot{V}O_2$ , some authors (56, 57) have proposed that its kinetics imply two components: a rapid "cardiodynamic" phase (phase I), due to potential transitory effects of an immediate cardiac response on  $\dot{V}O_2$  during the earliest seconds of exercise, followed by a slower monoexponential increase (phase II), related to the metabolic adaptations in contracting skeletal muscles. This view restricts the correspondence between lung O<sub>2</sub> uptake and muscle O<sub>2</sub> consumption to the monoexponential phase II. Perhaps the strongest piece of evidence in support of the phase I concept is the finding that the kinetics of cardiac output ( $\dot{Q}$ ) upon light exercise onset is much faster than that of  $\dot{V}O_2$  (12, 14, 21, 34, 38, 59, 60). In fact, assuming invariant O<sub>2</sub> concentration in mixed venous blood in the first seconds of exercise, this finding would imply, according to the Fick principle, a corresponding rapid increase in  $\dot{V}O_2$ .

As far as  $\dot{Q}aO_2$  is concerned, it can clearly be hypothesized that its kinetics during light exercise may, in fact, be faster than that of  $\dot{V}O_2$ . If we assume that  $CaO_2$  remains unchanged also in the exercise transient, as normoxic subjects operate about the flat portion of the O<sub>2</sub> dissociation curve, then the kinetics of  $\dot{Q}aO_2$  would have to be similar to that of  $\dot{Q}$ . Therefore, because of the rapid  $\dot{Q}$  kinetics, the  $\dot{Q}aO_2$  kinetics is expected to be much faster than that of  $\dot{V}O_2$ . To the best of our knowledge, however, the kinetics of  $\dot{Q}aO_2$  on exercise onset has yet to be determined in humans. The kinetics of femoral artery O<sub>2</sub> flow was determined during single-leg exercise and found to be only slightly faster than that of leg  $\dot{V}O_2$  during single-leg exercise in humans (27), in contrast with what may be expected at the systemic level.

In this study, we aimed to make simultaneous determinations of  $\dot{Q}aO_2$  and  $\dot{Q}$  on a beat-by-beat basis, for the first time,

Address for reprint requests and other correspondence: G. Ferretti, Département de Physiologie, Centre Médical Universitaire, 1 rue Michel Servet, 1211 Genève 4, Switzerland (e-mail: guido.ferretti@medecine.unige.ch).

The costs of publication of this article were defrayed in part by the payment of page charges. The article must therefore be hereby marked "advertisement" in accordance with 18 U.S.C. Section 1734 solely to indicate this fact.



in conjunction with breath-by-breath  $\dot{V}O_2$  in the same human subjects. We, therefore, tested at the whole body level whether at the onset of light aerobic exercise 1) the kinetics of  $\dot{Q}aO_2$  were, indeed, faster than that of  $\dot{V}O_2$  and 2) the kinetics of  $\dot{Q}aO_2$  had, indeed, the same time constants as that of  $\dot{Q}$ . Furthermore, because the two-component model of  $\dot{V}O_2$  kinetics (56, 57) requires a close quantitative correspondence between  $\dot{Q}$  and  $\dot{V}O_2$  in the first phase of the transient, this experiment allowed us to also test whether or not the changes in amplitude of the  $\dot{Q}$  explained entirely the corresponding  $\dot{V}O_2$  increase in the first phase.

## METHODS

**Subjects.** Six healthy nonsmoking young male subjects took part in the experiments. They were  $24.2 \pm 3.2$  yr old and weighed  $83.2 \pm 12.5$  kg. Their maximal  $O_2$  consumption in normoxia was  $4.44 \pm 0.56$  l/min. Their maximal aerobic power was  $333 \pm 61$  W. All subjects were informed about the procedures and the potential risks of the experiments, and all of them signed an informed consent form. The local Ethics Committee reviewed and approved the study.

**Measurements.**  $\dot{V}O_2$  was determined at the mouth on a breath-by-breath basis. The time course of  $O_2$  and  $CO_2$  partial pressures throughout the respiratory cycles were continuously monitored by a mass spectrometer (Balzers Prisma, Balzers, Liechtenstein) and calibrated against gas mixtures of known composition. The inspiratory and expiratory ventilations were measured by an ultrasonic flowmeter (Spiroson, Ecomedics, Duernten, Switzerland) calibrated with a 3-liter syringe. The alignment of the traces was corrected for the time delay between the flowmeter and the mass spectrometer. Breath-by-breath  $\dot{V}O_2$  and  $CO_2$  output ( $\dot{V}CO_2$ ) were then computed by means of the Grönlund's algorithm (8). A software specifically written under the Labview developing environment was used.

Heart rate ( $f_{Hr}$ ) and arterial  $O_2$  saturation ( $Sa_{O_2}$ ) were continuously measured by electrocardiography (Elmed ETM 2000; Augsburg, Germany) and by fingertip infrared oximetry (Ohmeda 2350; Finapres, Madison, WI), respectively. Continuous recordings of arterial pulse pressure were obtained at a fingertip of the right arm by means of a noninvasive cuff pressure recorder (Portapres, TNO, Eindhoven, The Netherlands). Beat-by-beat mean arterial pressure ( $\dot{Q}$ ) was computed as the integral mean of each pressure profile, using the Beatscope software package (TNO).

The stroke volume of the heart ( $Q_{St}$ ) was determined on a beat-by-beat basis by means of the model flow method (55), applied off-line to the pulse pressure profiles, using again the Beatscope software package. Beat-by-beat  $\dot{Q}$  was computed as the product of single beat  $Q_{St}$  times the corresponding single beat  $f_{Hr}$ . Each beat-by-beat  $\dot{Q}$  value was then corrected for a proportionality factor to account for the method's inaccuracy (2). To this end, steady-state  $\dot{Q}$  values were obtained also by means of the open-circuit acetylene method (3). In practice, at rest and at *minute 7* of each exercise period, the subject inhaled a normoxic gas mixture containing 1% acetylene and 5% helium for at least 20 respiratory cycles. During this measurement, inspired air was administered from precision high-pressure gas cylinders via an 80-liter Douglas bag buffer. The gas flow from the cylinders was adjusted to the subject's ventilation. For each subject, the partition coefficient for acetylene was determined on a different occasion by mass spectrometry (36), on 5-ml venous blood samples. Individual correction factors at rest and at each workload were calculated by dividing the  $\dot{Q}$  values obtained with the open-circuit acetylene technique by the corresponding average  $\dot{Q}$  values obtained with the model flow method. ANOVA showed no effect of exercise on the correction factor ( $P > 0.05$ ) but significant differences among subjects ( $P < 0.05$ ). Thus individual mean correction factors were used, on the assumption of no significant changes of them during the

exercise transients. Correction factors ranged between 0.98 and 1.47 (mean  $1.264 \pm 0.187$ ).

Exercise was carried out on an electrically braked cycle ergometer (Ergometrics 800-S; Ergoline, Bitz, Germany). The pedaling frequency was recorded, and its sudden increase at the exercise onset and decrease at the exercise offset were used as markers to identify precisely the start and the end of exercise. The electromechanical characteristics of the ergometer were such as to permit workload application in  $<50$  ms.

All of the signals were digitized in parallel by a 16-channel A/D converter (model MP 100; Biopac Systems, Santa Barbara, CA) and stored on a computer. The acquisition rate was 100 Hz.

Blood hemoglobin concentration, [Hb], was measured by a photometric technique (HemoCue, Angelholm, Sweden) on 10- $\mu$ l blood samples from a peripheral venous line inserted into the left forearm. Blood lactate concentration, [La]<sub>b</sub>, was measured by an electroenzymatic method (Eppendorf EBIO 6666, Hamburg, Germany) on 20- $\mu$ l blood samples from the same venous line. Arterial blood gas composition was measured by microelectrodes (Synthesis 10; Instrumentation Laboratory, Milano, Italy) on 300- $\mu$ l blood samples taken from an arterial catheter inserted in the left radial artery.

**Protocol.** After performance of blood sampling and measurement of acetylene cardiac output at rest, 2 min of quiet rest was allowed. Then, the exercise at 50 W started, lasting for 10 min. Arterial blood gas composition and [La]<sub>b</sub> were measured at *minute 5* and at the end of exercise. At *minute 7*, the acetylene cardiac output was measured. The 50-W exercise was followed by a 10-min recovery period, during which [La]<sub>b</sub> was measured at *minutes 2, 4, and 6*, and arterial blood gas composition was determined at *minutes 5 and 10*. Then, the 100-W exercise was carried out, for a 10-min duration, and with the same timing of events as at 50 W. A 10-min recovery followed, with the same characteristics as for the previous one. The overall duration of this protocol was about 50 min, during which [Hb] was systematically measured at 1-min intervals.

Each subject repeated this protocol four times. At each repetition, the performance of blood sampling for [Hb] determination was shifted by 15 s without changing the 1-min interval between successive measurements, so that, for *repetitions 1, 2, 3, and 4*, respectively, the first [Hb] determination took place at overall protocol time 0, 15, 30, and 45 s, the second at overall protocol time 60, 75, 90, and 105 s, and so on until the end of an experimental session. When the four tests were superimposed, this time shift allowed an overall description of the changes in [Hb] on a 15-s time basis.

**Data treatment.** The superimposed time course of [Hb] was smoothed by a four-sample mobile mean, to account for interrepetition variability, and interpolated by means of a 6th degree polynomial.  $Sa_{O_2}$  was averaged among the four repetitions and interpolated by means of a 6th degree polynomial. The resulting functions, describing the time course of [Hb] and  $Sa_{O_2}$ , were used to compute the time course of arterial  $O_2$  concentration ( $Ca_{O_2}$ , ml/l), on an equivalent beat-by-beat time scale, established after the pulse pressure profile traces, as

$$Ca_{O_2}(t) = Sa_{O_2}(t) * [Hb](t) * \sigma \quad (1)$$

where constant  $\sigma$  (1.34 ml/g) is the physiological  $O_2$  binding coefficient of hemoglobin, and time ( $t$ ) corresponds to the time of each heart beat.

The beat-by-beat  $f_{Hr}$ ,  $Q_{St}$ ,  $P$ , and  $\dot{Q}$  values from the four repetitions were aligned temporally, by setting the time of exercise start or stop as *time 0* for the analysis of on- and off-kinetics, respectively. Then they were averaged on a beat-by-beat basis to obtain a single averaged superimposed time series for each parameter. Beat-by-beat  $\dot{Q}aO_2$  was then calculated as

$$\dot{Q}aO_2(t) = \dot{Q}(t) * Ca_{O_2}(t) \quad (2)$$

Beat-by-beat total peripheral resistance ( $R_p$ ) was calculated by dividing each value of  $P$  by the corresponding  $\dot{Q}$  value, on the assumption



that the pressure in the right atrium can be neglected as a determinant of peripheral resistance.

The breath-by-breath  $\dot{V}_{O_2}$  values were interpolated to 1-s intervals (30). Then the four repetitions were aligned temporally, as described above, and averaged to obtain a single averaged superimposed time series also for  $\dot{V}_{O_2}$ .

**Models.** Several authors have proposed that the kinetics of  $\dot{V}_{O_2}$  during light or moderate exercise, hindered by the inertia of the metabolic activation at the onset of muscle contraction, is conveniently described by a single capacitance model (5, 19). Within this context, and thus assuming that  $\dot{V}_{O_2}$  reflects closely muscle  $O_2$  consumption, so that it is legitimate to infer from the former on the latter, the  $\dot{V}_{O_2}$ ,  $\dot{Q}$ , and  $\dot{Q}a_{O_2}$  kinetics at the onset of exercise would be described by the following monoexponential equations, respectively

$$\dot{V}_{O_2}(t) = \dot{V}_{O_2,ss}(1 - e^{-kt}) \quad (3a)$$

$$\dot{Q}(t) = \dot{Q}_{ss}(1 - e^{-kt}) \quad (3b)$$

$$\dot{Q}a_{O_2}(t) = \dot{Q}a_{O_2,ss}(1 - e^{-kt}) \quad (3c)$$

where suffix ss indicates the average steady state value (net value above resting), and  $k$  is the velocity constant for the parameter at stake—note that  $k$  is the reciprocal of the time constant  $\tau$ .

Some authors have proposed an alternative to the single capacitance model; it is a more complex model (4, 56), defined here as the two-phase model, whereby an exponential increase in flow (phase II), related to metabolic adaptation in skeletal muscle, is preceded by a faster flow increase in the first seconds of exercise (phase I), which Barstow and Molé (4) treated as an exponential. In the context of this model, the net  $\dot{V}_{O_2}$  kinetics upon exercise onset is described by

$$\dot{V}_{O_2}(t) = A_1(1 - e^{-k_1t}) + H(t - d)A_2(1 - e^{-k_2(t-d)}) \quad (4a)$$

where  $k_1$  and  $k_2$  are the velocity constants of the exponential parameter ( $\dot{V}_{O_2}$  in this case) increase in phase I and II, respectively,  $d$  is the time delay, and  $A_1$  and  $A_2$  are the amplitude of the parameter increase during phase I and phase II, respectively.  $H(t - d)$  is the Heaviside function defined as

$$H(t - d) = \begin{cases} 0 & \text{if } t < d \\ 1 & \text{if } t \geq d \end{cases}$$

In the context of the same model, by analogy, the kinetics of  $\dot{Q}$  and  $\dot{Q}a_{O_2}$  at the onset of exercise are described by

$$\dot{Q}(t) = A_1(1 - e^{-k_1t}) + H(t - d)A_2(1 - e^{-k_2(t-d)}) \quad (4b)$$

$$\dot{Q}a_{O_2}(t) = A_1(1 - e^{-k_1t}) + H(t - d)A_2(1 - e^{-k_2(t-d)}) \quad (4c)$$

**Statistics.** At the steady state, data are given as means  $\pm$  SD. The effects of exercise intensity on the investigated parameters was analyzed by one-way ANOVA. A post hoc Bonferroni test was used to determine differences between pairs. Normal distribution of errors was assumed. The results were considered significant if  $P < 0.05$ .

During transients, the characteristic parameters of the two analyzed models were estimated by means of a weighted nonlinear least squares procedure (9), implemented in the commercial software Labview 5.0 (National Instruments, Austin, TX). Initial guesses of the parameters of the model were entered after visual inspection of the data. The characteristic parameters are given as means  $\pm$  SD. A nonparametric Wilcoxon test for paired observations was used 1) to evaluate the effects of exercise on the time constants of  $\dot{V}_{O_2}$ ,  $\dot{Q}$ , and  $\dot{Q}a_{O_2}$  and 2) to perform a comparison of the time constants of  $\dot{V}_{O_2}$ ,  $\dot{Q}$ , and  $\dot{Q}a_{O_2}$  at each of the investigated workloads. The results were considered significant if  $P < 0.05$ .

Intersubject variability and effects of exercise intensity on the correction factor for beat-by-beat determination of  $\dot{Q}$  were evaluated with the Kruskal-Wallis test (13).

**RESULTS**

The time courses of  $f_H$  and  $\dot{Q}$ , upon the onset of 50 W and 100 W exercises are shown in Figs. 1 and 2, respectively. All of these parameters increased upon exercise onset to reach a new steady state. The time course of  $\bar{P}$  and  $R_p$  upon the onset of 50 W and 100 W exercise are jointly reported in Fig. 3. At exercise start, there was a sudden decrease in  $\bar{P}$ , followed by a rapid increase, this within the first 20 s of exercise: at 100 W, this increase was such as to lead to a  $\bar{P}$  overshoot. Afterward,  $\bar{P}$  increased progressively, to attain a steady-state value higher than resting.  $R_p$  decreased very rapidly at exercise start, to reach a new steady-state value lower than at rest.

A contour plot, representing beat-by-beat  $f_H$  as a function of beat-by-beat  $\bar{P}$ , is shown in Fig. 4. The resting values are located on the lower-left side of the plot; the exercise steady-state values are located on the upper-right side. The pattern of displacement of the  $f_H$  vs  $\bar{P}$  operational site from rest to exercise is characterized by a rapid increase in  $f_H$  correcting the sudden  $\bar{P}$  fall at exercise start. This is translated into a shift leftward and upward of the relationship between  $f_H$  and  $\bar{P}$  that precedes the rightward shift toward the new baroreflex operational site.

Resting  $Sa_{O_2}$  was  $0.967 \pm 0.010$ , and resting  $Ca_{O_2}$  was  $192.9 \pm 11.4$  ml/l. At the exercise steady state,  $Sa_{O_2}$  was

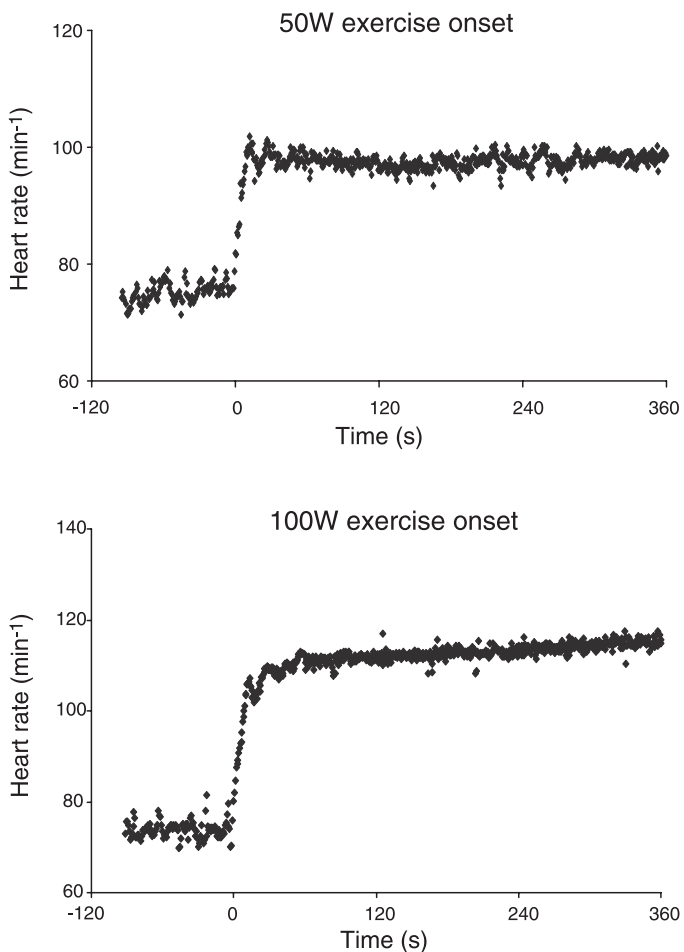


Fig. 1. Time course of heart rate upon the onset of exercise. Each value is the mean of the averaged superimposed values of all subjects. Time 0 corresponds to start of exercise.

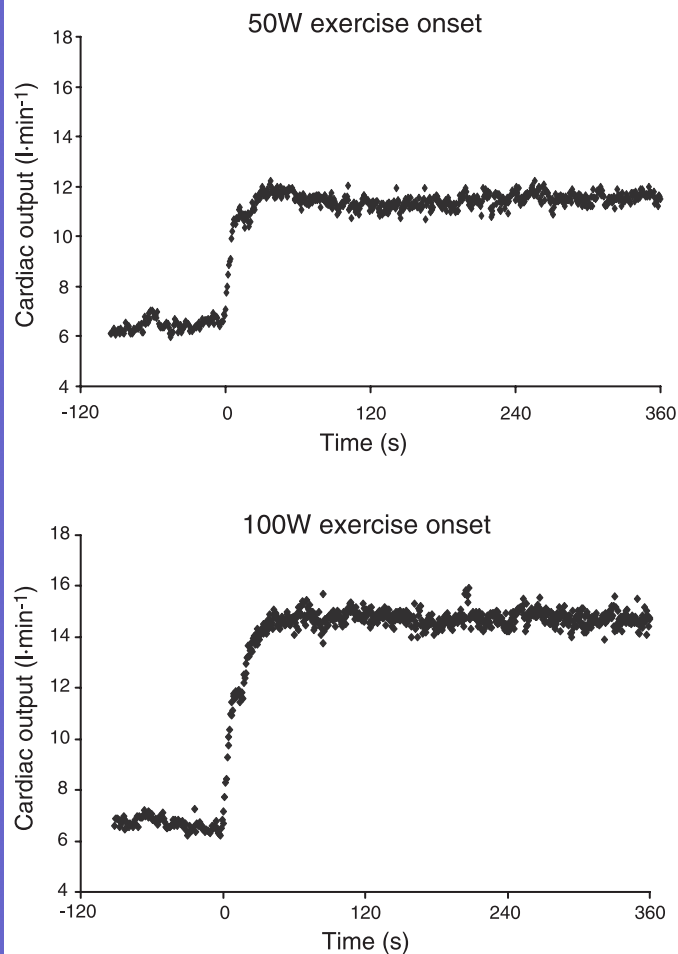


Fig. 2. Time course of cardiac output upon the onset of exercise. Each value is the mean of the averaged superimposed values of all subjects. *Time 0* corresponds to start of exercise.

0.965 ± 0.006 and 0.955 ± 0.011, at 50 W and 100 W, respectively.  $\text{CaO}_2$  was 194.0 ± 7.9 ml/l and 198.0 ± 8.3 ml/l, at 50 W and 100 W, respectively. The time course of  $\text{CaO}_2$  is shown in Fig. 5. Since  $\text{SaO}_2$  was unchanged, the evolution of  $\text{CaO}_2$  followed the changes in [Hb]. These changes were relatively slow with respect to the events occurring in the exercise transient. Arterial blood gas composition and pH are shown in Table 1 together with  $[\text{La}]_b$ . No significant differences among workloads were observed for any of these parameters.

The time courses of  $\dot{Q}a\text{O}_2$  and  $\dot{V}\text{O}_2$  upon the onset of 50 W and 100 W exercises are jointly reported in Fig. 6. To facilitate a comparison of the two parameters, data has been expressed in relative terms, whereby resting values were set equal to 0 and steady-state values were set equal to 100%. Both  $\dot{Q}a\text{O}_2$  and  $\dot{V}\text{O}_2$  increased upon exercise onset to reach a new steady state and decreased upon exercise offset to return to the respective resting values. However, the rate of readjustment of  $\dot{Q}a\text{O}_2$  at exercise onset appeared to be faster than that of  $\dot{V}\text{O}_2$ .

Resting and exercise steady-state mean values for  $\dot{Q}$ ,  $f_{\text{H}}$ ,  $Q_{\text{st}}$ ,  $\dot{Q}a\text{O}_2$ ,  $\dot{V}\text{O}_2$ ,  $\bar{P}$ , and  $R_p$ , are reported in Table 2. Mean  $\dot{Q}$ ,  $f_{\text{H}}$ ,  $Q_{\text{st}}$ ,  $\dot{Q}a\text{O}_2$  and  $\dot{V}\text{O}_2$  were higher at 50 W exercise than at rest, and at 100 W exercise than at 50 W.  $\bar{P}$  was higher at exercise than at rest. However, because its increase was smaller than that in  $\dot{Q}$ ,  $R_p$  resulted lower at exercise than at rest.

The characteristic parameters describing the  $\dot{Q}$ ,  $\dot{Q}a\text{O}_2$ , and  $\dot{V}\text{O}_2$  kinetics at exercise onset are presented in Tables 3 and 4, for the single capacitance and the two-phase models, respectively. With both models the time constants for  $\dot{Q}$  and  $\dot{Q}a\text{O}_2$  were not significantly different between them and resulted twice as fast as those for  $\dot{V}\text{O}_2$  ( $P < 0.05$ ).

**DISCUSSION**

In this study, we obtained simultaneous determinations of  $\dot{Q}a\text{O}_2$  and  $\dot{Q}$  on a beat-by-beat basis, for the first time, in

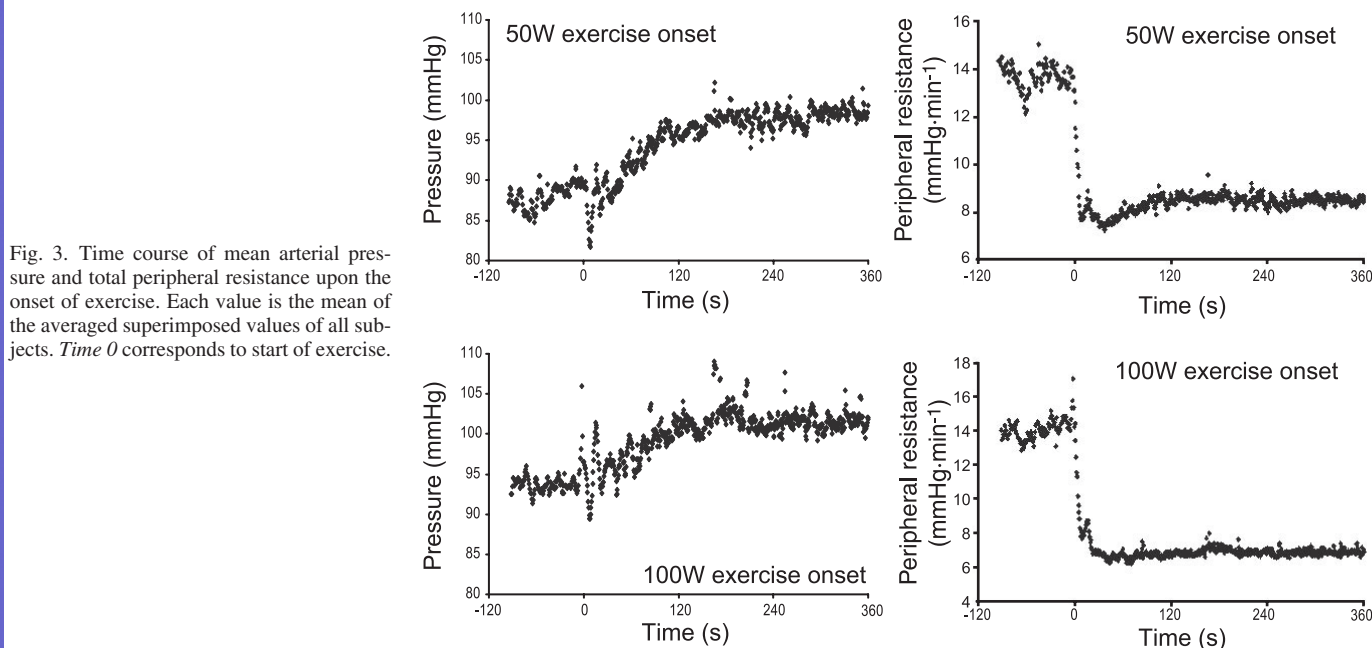


Fig. 3. Time course of mean arterial pressure and total peripheral resistance upon the onset of exercise. Each value is the mean of the averaged superimposed values of all subjects. *Time 0* corresponds to start of exercise.

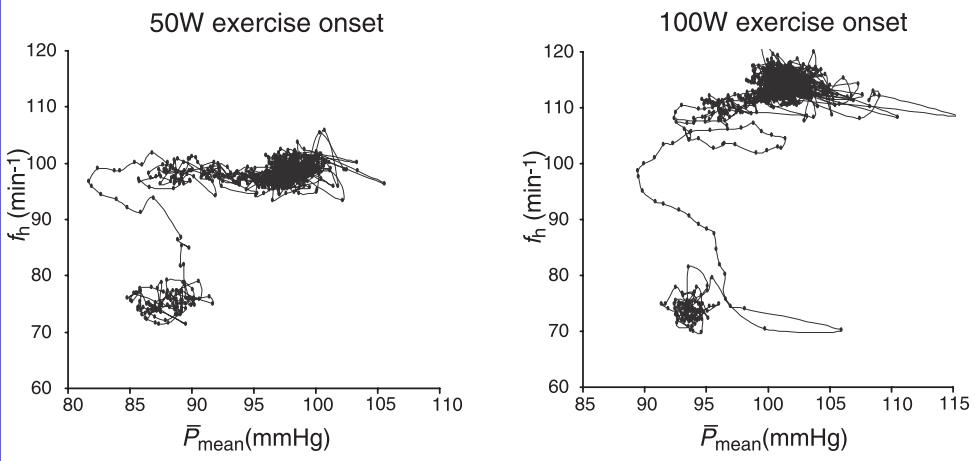


Fig. 4. Beat-by-beat heart rate as a function of the corresponding beat-by-beat mean arterial pressure upon the onset of 50 W and 100 W exercise. *Bottom, left* of each plot: resting values. *Top, right* of each plot: exercise steady-state values.  $f_H$ , heart rate;  $\bar{P}_{mean}$ , mean arterial pressure. The pattern of displacement of the  $f_H$  vs.  $\bar{P}_{mean}$  operational range from rest to exercise is completed within 20 beats at 50 W and 40 beats at 100 W.

conjunction with breath-by-breath  $\dot{V}O_2$  in the same human subjects. The main findings were that 1) the kinetics of  $\dot{Q}$  was twice as fast as that of  $\dot{V}O_2$ , no matter what model was applied; 2) the kinetics of  $\dot{Q}aO_2$  had the same time constants as that of  $\dot{Q}$ , no matter what model was applied, because  $CaO_2$  oscillations were so slow that  $CaO_2$  remained essentially unchanged during the first minute of exercise, in agreement with previous reports (27); and 3) using a two-phase model, the amplitude of

phase I  $\dot{Q}$  changes could fully explain the ensuing amplitude of phase I  $\dot{V}O_2$  increase. The first of these findings is consistent with and provides quantitative support to previous observations of a fast increase in  $\dot{Q}$  upon exercise onset (12, 14, 21, 38, 59, 60). The second finding demonstrates that the kinetics of  $\dot{Q}aO_2$  is indeed dictated by that of  $\dot{Q}$ , thus being by far faster than that of  $\dot{V}O_2$ . So this finding does not support the assumptions of the single capacitance model for  $\dot{V}O_2$  kinetics on exercise onset and suggests a potential dissociation between  $\dot{V}O_2$  and muscle  $O_2$  consumption in unsteady states. The third finding provides full quantitative support to the notion of a  $\dot{Q}$ -dependent phase I of the  $\dot{V}O_2$  kinetics.

*Methodological considerations.* The highest workload imposed to the subjects was <40% of their maximal aerobic power. There was no significant increase in  $[La]_b$  during exercise, whereas pH and  $PaCO_2$  values were not significantly different from resting (Table 1). As a consequence, all exercise was carried out below the so-called anaerobic threshold, and early lactate accumulation during the exercise transients (11) and the appearance of a third phase of the  $\dot{V}O_2$  kinetics characterized by a continuous increase in  $\dot{V}O_2$  and  $f_H$  (7, 58) were avoided.

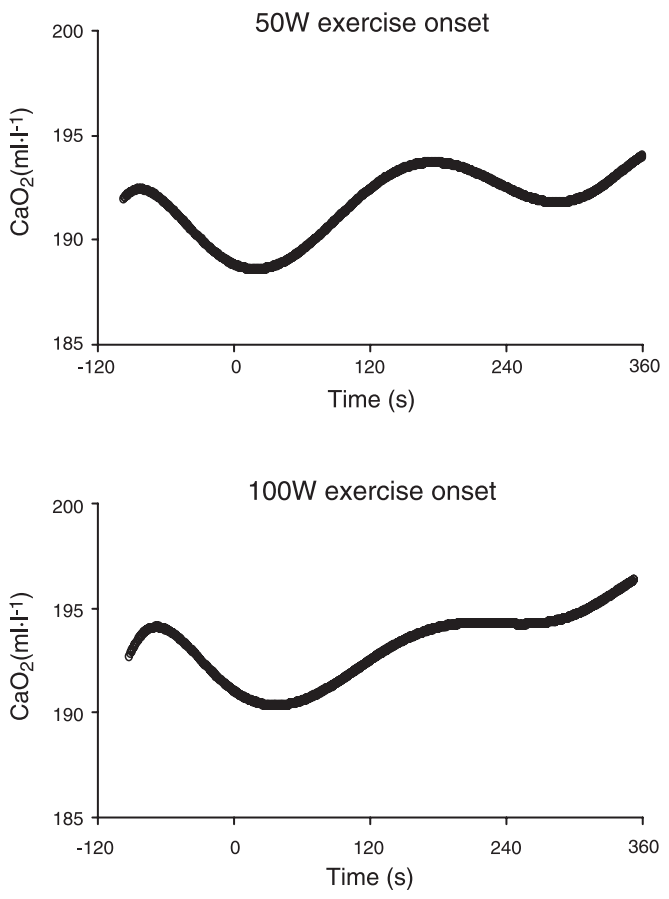


Fig. 5. Arterial  $O_2$  concentration upon the onset of exercise. The time course of arterial  $O_2$  concentration ( $CaO_2$ ) was calculated from the interpolation functions describing the time courses of hemoglobin concentration and arterial  $O_2$  saturation. The reported curve for 50 and 100 W exercise onset refers to the average superimposed function for all subjects.

Table 1. Blood lactate, arterial blood gas composition and arterial pH

|                   | pH          | $PaO_2$ , mmHg | $PaCO_2$ , mmHg | $[La]_b$ , mmol/l |
|-------------------|-------------|----------------|-----------------|-------------------|
| Rest              | 7.425±0.016 | 91.0±3.9       | 36.6±2.1        | 1.32±0.27         |
| 50 W (5 min)      | 7.412±0.013 | 89.6±2.0       | 38.2±2.5        | 1.18±0.18         |
| 50 W (10 min)     | 7.417±0.009 | 90.1±1.9       | 37.8±1.0        | 1.11±0.17         |
| Recovery (2 min)  |             |                |                 | 1.32±0.25         |
| Recovery (4 min)  |             |                |                 | 1.29±0.19         |
| Recovery (5 min)  | 7.418±0.015 | 88.9±3.1       | 37.2±1.9        |                   |
| Recovery (6 min)  |             |                |                 | 1.24±0.15         |
| Recovery (10 min) | 7.415±0.014 | 88.5±3.7       | 37.2±1.6        | 1.09±0.17         |
| 100W (5 min)      | 7.401±0.018 | 87.1±3.2       | 38.7±2.6        | 1.61±0.68         |
| 100W (10 min)     | 7.405±0.017 | 87.9±1.9       | 38.3±1.9        | 1.56±0.71         |
| Recovery (2 min)  |             |                |                 | 1.50±0.39         |
| Recovery (4 min)  |             |                |                 | 1.43±0.31         |
| Recovery (5 min)  | 7.417±0.009 | 90.2±3.4       | 36.7±1.6        |                   |
| Recovery (6 min)  |             |                |                 | 1.32±0.31         |
| Recovery (10 min) | 7.414±0.011 | 87.8±3.6       | 36.9±2.0        |                   |

Data are given as means ± SD.  $PaO_2$ , arterial  $O_2$  partial pressure;  $PaCO_2$ , arterial carbon dioxide partial pressure;  $[La]_b$ , blood lactate concentration.



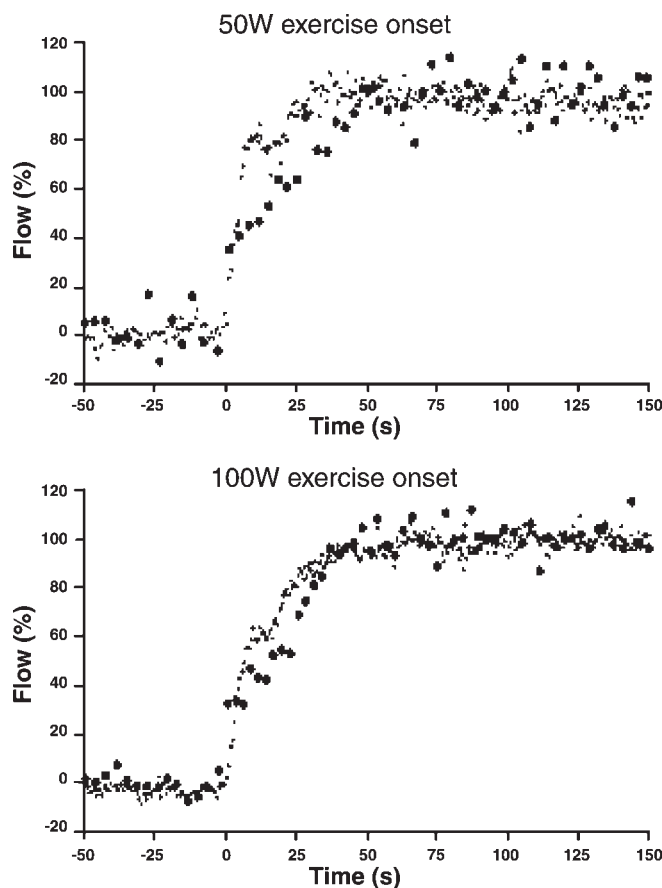


Fig. 6. Time course of systemic  $O_2$  delivery and  $O_2$  uptake at onset of exercise. Each value is the mean of the averaged superimposed values of all subjects. *Time 0* corresponds to start of exercise. Data are expressed in relative terms, whereby the mean resting value is set equal to 0 and the mean exercise steady-state value is set equal to 100%. Solid dots refer to systemic  $O_2$  delivery; Open dots refer to  $O_2$  uptake.

Breath-by-breath  $\dot{V}O_2$  was computed by the Grønlund algorithm (8). Indeed, classical algorithms for single-breath determination of alveolar gas exchange, all based on the concepts originally introduced by Auchincloss et al. (1), require the assumption of a fixed value for the end-expiratory alveolar volume. This assumption was demonstrated to increase the variability of breath-by-breath  $\dot{V}O_2$  assessment (18). Grønlund circumvented this problem by making the  $\dot{V}O_2$  computation algorithm independent of the end-expiratory alveolar volume

Table 2. Steady state values of cardiopulmonary parameters at rest, 50 W, and 100 W exercise

| Workload                          | Rest         | 50 W         | 100 W        |
|-----------------------------------|--------------|--------------|--------------|
| $\dot{Q}$ , l/min                 | 6.49 ± 0.18  | 11.79 ± 0.22 | 14.47 ± 0.24 |
| $f_H$ , per min                   | 70.7 ± 1.4   | 93.3 ± 1.3   | 113.5 ± 1.2  |
| $Q_{st}$ , ml                     | 83.7 ± 2.3   | 113.5 ± 1.8  | 128.4 ± 2.6  |
| $\dot{Q}_{aO_2}$ , l/min          | 1.08 ± 0.04  | 1.96 ± 0.04  | 2.29 ± 0.04  |
| $\dot{V}O_2$ , l/min              | 0.56 ± 0.05  | 1.45 ± 0.07  | 1.74 ± 0.06  |
| $\bar{P}$ , mmHg                  | 89.2 ± 1.7   | 98.9 ± 1.1   | 103.0 ± 1.2  |
| $R_p$ , mmHg·min <sup>-1</sup> ·l | 13.83 ± 0.51 | 8.57 ± 0.21  | 6.99 ± 0.17  |

Data are given as means ± SD of single beat values over 1 min at rest and exercise steady state.  $\dot{Q}$ , cardiac output;  $f_H$ , heart rate;  $Q_{st}$ , stroke volume;  $\dot{Q}_{aO_2}$ , systemic  $O_2$  delivery;  $\dot{V}O_2$ ,  $O_2$  uptake;  $\bar{P}$ , mean arterial pressure;  $R_p$ , peripheral resistance.

Table 3. The kinetics of cardiac output, systemic  $O_2$  delivery and  $O_2$  uptake within the single capacitance model

|                  | $k$ , per s   | $\tau$ , s   |
|------------------|---------------|--------------|
| 50 W             |               |              |
| $\dot{Q}$        | 0.233 ± 0.148 | 6.35 ± 4.19  |
| $\dot{Q}_{aO_2}$ | 0.200 ± 0.131 | 6.89 ± 4.07  |
| $\dot{V}O_2$     | 0.061 ± 0.008 | 16.57 ± 1.85 |
| 100 W            |               |              |
| $\dot{Q}$        | 0.079 ± 0.010 | 12.81 ± 1.67 |
| $\dot{Q}_{aO_2}$ | 0.075 ± 0.010 | 13.54 ± 1.92 |
| $\dot{V}O_2$     | 0.054 ± 0.007 | 18.75 ± 2.50 |

Data are given as means ± SD.  $k$ , velocity constant;  $\tau$ , time constant.

(28). Grønlund's algorithm was validated at rest and at the exercise steady state against the standard open circuit method and against numerous algorithms derived from Auchincloss; it was demonstrated to provide the same steady-state values, yet with much less variability around the mean value than for any other tested algorithm (8). Furthermore, a comparative analysis of algorithms derived from Auchincloss during exercise transients demonstrated a linear relationship between end-expiratory lung volume and phase II time constant of  $O_2^-$  kinetics, allowing the conclusion that these algorithms generate spurious  $\dot{V}O_2$  kinetics at the onset of exercise, whereas the time constants provided by Grønlund's algorithm were systematically faster than with any other algorithm (10). Thus Grønlund's algorithm increases the precision of single-breath  $\dot{V}O_2$  assessment and allows more accurate estimates of the  $\dot{V}O_2$  kinetics during step exercise transients.

$\dot{Q}$  was measured by application of the model flow method to pulse pressure profiles obtained noninvasively from a fingertip artery. The method assumes impedance characteristics of the arterial wall of the aorta (31), whereas fingertip pressure profiles are typical of peripheral arteries. This discrepancy causes lower absolute pressure values and inaccurate  $\dot{Q}$  values (2, 25). To use this method for obtaining beat-by-beat  $\dot{Q}$  values, a correction for an established steady-state method simultaneously applied on the same subjects must be carried out. This justifies the simultaneous performance of  $\dot{Q}$  measurements by the open circuit acetylene technique in this study and the application of a correction procedure, as previously described (49). Calculated correction factors did not differ significantly among both workloads and subjects. This allowed application of an overall correction factor of 1.264, which turned out to be similar to that previously reported with the same techniques (49). After correction, model flow  $\dot{Q}$  computation can be conveniently applied also during dynamic states with rapid changes in  $\dot{Q}$  (51).

[Hb] cannot be measured continuously or on a beat-by-beat basis, as required by the computation of beat-by-beat  $\dot{Q}_{aO_2}$ . We had [Hb] determinations at 1-min intervals, and the 15-s shift in blood sampling from one repetition to the other allowed to obtain, across repetitions, [Hb] values at 15-s intervals. These values, however, are affected by the intrinsic variability of [Hb] from one day to the other, which was dealt with by applying a mobile mean smoothing technique over four [Hb] values. Interpolation allowed the construction of a function, whereby the time course of [Hb] was estimated. In so doing, estimated [Hb], and thus  $Ca_{O_2}$ , values at the time of each heart

Table 4. *The kinetics of systemic O<sub>2</sub> delivery, O<sub>2</sub> uptake, and cardiac output within the two-phase model*

|                  | A <sub>1</sub> , l/min | A <sub>2</sub> , l/min | d, s         | k <sub>1</sub> , per s | k <sub>2</sub> , per s | τ <sub>1</sub> , s | τ <sub>2</sub> , s |
|------------------|------------------------|------------------------|--------------|------------------------|------------------------|--------------------|--------------------|
| 50 W             |                        |                        |              |                        |                        |                    |                    |
| Q                | 4.35 ± 0.62            | 1.41 ± 0.73            | 20.84 ± 2.78 | 0.381 ± 0.130          | 0.589 ± 0.389          | 3.02 ± 1.50        | 2.10 ± 1.04        |
| QaO <sub>2</sub> | 0.69 ± 0.07            | 0.30 ± 0.23            | 22.82 ± 7.15 | 0.429 ± 0.154          | 0.541 ± 0.347          | 2.69 ± 1.31        | 2.54 ± 1.48        |
| ṠO <sub>2</sub>  | 0.36 ± 0.15            | 0.60 ± 0.18            | 12.14 ± 5.90 | 4.070 ± 3.689          | 0.065 ± 0.005          | 0.54 ± 0.57        | 15.38 ± 1.15       |
| 100 W            |                        |                        |              |                        |                        |                    |                    |
| Q                | 5.07 ± 1.01            | 3.03 ± 0.33            | 15.70 ± 2.15 | 0.380 ± 0.166          | 0.136 ± 0.062          | 3.10 ± 1.42        | 8.53 ± 3.28        |
| QaO <sub>2</sub> | 0.73 ± 0.17            | 0.54 ± 0.11            | 15.65 ± 4.20 | 0.875 ± 1.107          | 0.129 ± 0.053          | 2.47 ± 1.64        | 9.29 ± 4.60        |
| ṠO <sub>2</sub>  | 0.48 ± 0.14            | 0.82 ± 0.18            | 15.55 ± 2.86 | 1.319 ± 0.782          | 0.061 ± 0.006          | 1.40 ± 1.57        | 16.56 ± 1.86       |

Data are given as means ± SD. A<sub>1</sub>, amplitude of phase I change; A<sub>2</sub>, amplitude of phase II change; d, time delay of phase II; k<sub>1</sub>, velocity constant of phase I; k<sub>2</sub>, velocity constant of phase II; τ<sub>1</sub>, time constant of phase I; τ<sub>2</sub>, time constant of phase II.

beat could be attributed to the corresponding beat-by-beat  $\dot{Q}$  values, to compute beat-by-beat  $\dot{Q}aO_2$ .

**Cardiovascular adjustments during the exercise transient.** The rapid increase in  $\dot{Q}$  (Fig. 2) is the result of a number of regulatory mechanisms that are activated at exercise onset. As exercise starts, a strong and prompt decrease in  $R_p$  takes place (Fig. 3), with subsequent dramatic and fast increase in muscle or limb blood flow (23, 27, 44, 50, 52). Whatever the causes of the  $R_p$  fall—vasodilatation (myogenic, neurogenic, see Ref. 32) and/or muscle pump action (48), its immediate effect is the sudden, transient drop in P (Fig. 3). This P fall cannot be corrected for by an increase in  $f_{H_i}$  induced by arterial baroreflexes, because mean values of  $\bar{P}$  are at the margins, if not outside, the operational baroreflex range. Correction of  $\bar{P}$  requires more drastic responses. These would include an immediate resetting of baroreflexes (Fig. 4), as demonstrated at the exercise steady state (29, 39, 41, 43). Such a resetting may be driven either by the changes in  $R_p$  (40) or by afferent inputs from skeletal muscle receptors (42) or eventually anticipated by a kind of “central command” mechanism (24). Moreover, a withdrawal of the vagal drive to the heart occurs (22), which would explain the sudden step increase in  $f_{H_i}$  (Fig. 1). Finally, muscle and/or diaphragmatic pump action may lead to a sudden increase in venous return, with consequent corresponding increase in  $Q_{st}$  (data not shown in Figures) due to the Frank-Starling mechanism, as demonstrated in dogs (47).

Baroreflex resetting and withdrawal of vagal drive may, in fact, explain a great deal of the cardiovascular response at the onset of exercise (20) and design an overall on/off switch of the global regulation of the cardiovascular system, and perhaps also of the respiratory system, upon exercise onset. However, the resulting increase in  $\dot{Q}$  would not be possible without a concomitant immediate increase in venous return due to muscle pump action.

If this is so, the kinetics of  $\dot{Q}$  upon exercise onset would be better represented by a two-phase rather than a single capacitance model. The first, immediate, phase would account for baroreflex resetting, withdrawal of vagal drive, and increase in preload; the second, delayed and kinetically slower, phase might parallel sympathetic drive stimulation.

**Of the  $\dot{V}O_2$  and  $\dot{Q}aO_2$  on kinetics.** Application of the single capacitance model to the description of  $\dot{V}O_2$  kinetics relied on the assumption that, once possible changes in blood O<sub>2</sub> stored are accounted for, lung  $\dot{V}O_2$  reflects muscle O<sub>2</sub> consumption. This assumption implies that the time constant of  $\dot{V}O_2$  ought to be equal to that of muscle O<sub>2</sub> consumption, or of its mirror image, the muscle phosphocreatine decrease. This seemed to

be the case in previous studies (15, 33), in which algorithms based on Auchincloss’s principles were used (1). Furthermore, a correspondence between the time constant of  $\dot{V}O_2$  and that of muscle phosphocreatine decrease was reported in a study on single-leg extension exercise (45), further reinforcing this notion. In the present study, however, faster time constants for  $\dot{V}O_2$  were obtained than in previous studies (15, 33) with the same exercise mode and intensities. The present time constants for  $\dot{V}O_2$  were also faster than those found by others for the monoexponential phosphocreatine decrease upon exercise onset (6, 17, 45), a mirror image of muscle O<sub>2</sub> consumption independent of the exercise mode. These fast time constants, perhaps an intrinsic consequence of the improved computational method (10), suggest a lack of correspondence between lung  $\dot{V}O_2$  and muscle O<sub>2</sub> consumption.

On the other hand, the time constants of  $\dot{Q}$  and  $\dot{Q}aO_2$  were definitely faster than those of  $\dot{V}O_2$ . These findings reinforce the concept that the kinetics of  $\dot{Q}aO_2$  and of  $\dot{V}O_2$  are dissociated. If this is so, then changes in O<sub>2</sub> extraction should occur and an “early” effect of  $\dot{Q}aO_2$  on  $\dot{V}O_2$  should be seen, as originally postulated by Wasserman et al. (53) and modeled by Barstow and Molé (4). In fact, these authors assumed similar time constants for pulmonary blood flow as found in the present study for  $\dot{Q}$  and  $\dot{Q}aO_2$ . Extension of the single capacitance model to the description of the kinetics of  $\dot{Q}$  and  $\dot{Q}aO_2$  requires the assumption of a close matching of  $\dot{V}O_2$  to  $\dot{Q}aO_2$ . This assumption is not supported by the present results.

The kinetics of leg  $\dot{V}O_2$  and leg O<sub>2</sub> flow during single-leg exercise were also analyzed by means of a single capacitance model (27). The time constant of leg O<sub>2</sub> flow was found to be only slightly faster than that of the leg  $\dot{V}O_2$ , despite the well-known rapidity of muscle blood flow adaptation at exercise onset (23, 27, 44, 50, 52). Yet the present time constants for  $\dot{Q}$  and  $\dot{Q}aO_2$  were definitely faster than those reported for leg O<sub>2</sub> flow, suggesting that muscle O<sub>2</sub> transfer and systemic O<sub>2</sub> flow are the consequence of different, independent phenomena. More recently, on isolated, perfused dog gastrocnemii, the time constant of the  $\dot{V}O_2$  kinetics was found to be equal in conditions of normal and forced O<sub>2</sub> delivery and equal to that calculated for the kinetics of muscle phosphocreatine decrease (26), demonstrating an independent peripheral component of the kinetics of muscle O<sub>2</sub> consumption.

The results obtained with the two-phase model provided a phase I time constant of  $\dot{V}O_2$  kinetics that was extremely rapid and functionally instantaneous. This would correspond to a practically immediate upward translation of  $\dot{V}O_2$  visible since the first breath. Very fast time constants of phase I (Table 4)



were found also for the kinetics of  $\dot{Q}$  and  $\dot{Q}aO_2$ , compatible with the notion of immediate vagal withdrawal. These time constants cannot be considered different from those obtained for  $\dot{V}O_2$  as far as the minimal time window on which the  $\dot{V}O_2$  kinetics can be determined is one breath length. The results of the present analysis refine and support quantitatively the observation (12) of a close correspondence between the rapid increase of  $\dot{Q}$  and ventilation at exercise onset. For all parameters, the time constants of phase II were slower than those of phase I at 100 W, but at 50 W, they were as fast as those of phase I. At both workloads, phase II time constants of  $\dot{Q}$  and  $\dot{Q}aO_2$ , which may reflect slower sympathetic activation, remained by far faster than those of  $\dot{V}O_2$ , but the time delay was the same. Thus the phase II of the  $\dot{Q}aO_2$  kinetics would only partially explain the phase II of the  $\dot{V}O_2$  kinetics. Finally, the phase II time constants were slightly but significantly faster than those found within the single capacitance model, as a consequence of the introduction of a time delay. Nevertheless, the time constant of  $\dot{V}O_2$  in phase II resulted in faster time constants than reported (4, 57) in studies in which algorithms derived from Auchincloss et al (1) were used and remained faster than previously reported for muscle phosphocreatine decrease (6, 17, 45), suggesting again possible dissociation between lung  $O_2$  uptake and muscle  $O_2$  consumption.

In two cases at 50 W, phase II could not even be identified by the fitting procedure, and the overall kinetics of  $\dot{Q}$  was accounted for by a single component. Within the context of a two-phase model, this might have been the consequence of an initial  $\dot{Q}$  overshoot that perhaps concealed the second phase increase in  $\dot{Q}$ . Nevertheless, the question arises as to whether sympathetic activation really occurs during very low workloads, and thus as to whether a single capacitance model, with a very fast time constant, would provide a complete description of the events occurring in the cardiovascular system upon light exercise onset.

$\dot{Q}aO_2$  is the product of  $\dot{Q}$  times  $CaO_2$ .  $CaO_2$  variations paralleled those of [Hb] (Fig. 5) and were subject to slow oscillations, with a period ranging between 4 and 5 min. Within the time window of the exercise transients, even in the case of greatest oscillation amplitude (20 ml/l), the effects of these oscillations on  $CaO_2$  were at most 1% and thus introduced a practically negligible distortion of the  $\dot{Q}aO_2$  kinetics with respect to that of  $\dot{Q}$ . In fact, the time constants of the two phases of the  $\dot{Q}aO_2$  kinetics did not result significantly different from those of  $\dot{Q}$ . This allows the conclusion that the kinetics of  $\dot{Q}aO_2$  upon exercise onset is, indeed, dictated by that of  $\dot{Q}$ .

If we look at the Fick principle, it helps us understand whether the phase I of the  $\dot{Q}$  or  $\dot{Q}aO_2$  kinetics explains the phase I of the  $\dot{V}O_2$  kinetics at the mouth. Because of a delay between muscle  $O_2$  consumption and lung  $O_2$  uptake, we can reasonably assume that during the first seconds of exercise, the composition of mixed venous blood remains unchanged, and thus arterial-venous  $O_2$  difference ( $CaO_2 - CvO_2$ ) stays equal to that at rest (4, 54). This being so, any increase in  $\dot{V}O_2$  during phase I would be a consequence of an increase in  $\dot{Q}$  only. The amplitude of phase I  $\dot{Q}$  was on average 4.3 l/min (see Table 4). This amplitude, for an average resting  $CaO_2 - CvO_2$  of 87 ml/l, would produce a corresponding immediate  $\dot{V}O_2$  increase of 374 ml/min, which is very close to the observed amplitude of phase I for  $\dot{V}O_2$ , reported in Table 4 ( $355 \pm 148$  ml/min). This computation allows the conclusion that the amplitude of phase

I for  $\dot{V}O_2$  is indeed entirely accounted for by the  $\dot{Q}$  increase during phase I, in agreement with the hypothesis put forward by others (56, 57). This analysis further supports the notion of a possible dissociation between lung  $\dot{V}O_2$  and muscle  $O_2$  consumption.

In conclusion, the kinetics of  $\dot{Q}$  and  $\dot{Q}aO_2$  upon exercise onset were significantly faster than that of lung  $\dot{V}O_2$ , as expected. Consistent with the Fick principle, this finding implies a rapid component in the  $\dot{V}O_2$  kinetics. Application of a two-phase model showed that the amplitude of phase I  $\dot{V}O_2$  increase is entirely accounted for by the amplitude of phase I  $\dot{V}O_2$  increase. The second phase of the  $\dot{V}O_2$  kinetics is only partially related to the second phase of  $\dot{Q}$  and  $\dot{Q}aO_2$  kinetics. The kinetics of  $\dot{Q}aO_2$  is entirely dictated by the kinetics of  $\dot{Q}$ . The fast time constants of  $\dot{V}O_2$ , as well as the fast time constants of  $\dot{Q}aO_2$  in relation to  $\dot{V}O_2$ , suggest the potential dissociation between  $\dot{V}O_2$  and muscle  $O_2$  consumption in unsteady states. We speculate that  $\dot{V}O_2$  kinetics is under the influence of the systemic cardiovascular response to exercise, whereas only muscle  $O_2$  consumption kinetics is affected by the metabolic regulatory processes. This being the case, the two components of the cardiovascular response to exercise (phase I and phase II) may reflect vagal withdrawal and sympathetic activation, respectively.

#### ACKNOWLEDGMENTS

We thank Pietro Enrico di Prampero for fruitful discussions on the data.

#### GRANTS

This study was supported by Swiss National Science Foundation Grants 3200-061780 and 3200B0-102181 (to Guido Ferretti) and by Italian Space Agency Grant ASI I/R/300/02 (to Carlo Capelli).

#### REFERENCES

1. Auchincloss JH Jr, Gilbert R, and Baule GH. Effect of ventilation on oxygen transfer during early exercise. *J Appl Physiol* 21: 810–818, 1966.
2. Azabji Kenfack M, Lador F, Licker MJ, Moia C, Tam E, Capelli C, Morel D, and Ferretti G. Cardiac output by model flow method from intra-arterial and finger tip pulse pressure profiles. *Clin Sci* 106: 365–369, 2004.
3. Barker RC, Hopkins SR, Kellogg N, Olfert IM, Brutsaert, TD, Gavin TP, Entin PL, Rice AJ, and Wagner PD. Measurement of cardiac output by open-circuit acetylene technique. *J Appl Physiol* 87: 1506–1512, 1999.
4. Barstow TJ and Molé PA. Simulation of pulmonary  $O_2$  uptake during exercise transients in humans. *J Appl Physiol* 63: 2253–2261, 1987.
5. Binzoni T and Cerretelli PP. Muscle 31-P NMR in humans: estimate of bias and qualitative assessment of ATPase activity. *J Appl Physiol* 71: 1700–1704, 1991.
6. Binzoni T, Ferretti G, Schenker K, and Cerretelli P. Phosphocreatine hydrolysis by  $^{31}P$ -NMR at the onset of constant-load exercise. *J Appl Physiol* 73: 1644–1649, 1992.
7. Capelli C, Antonutto G, Zamparo P, Girardis M, and di Prampero PE. Effects of prolonged cycle ergometer exercise on maximal muscle power and oxygen uptake in humans. *Eur J Appl Physiol* 66: 189–195, 1993.
8. Capelli C, Cautero M, and di Prampero PE. New perspectives in breath-by-breath determination of alveolar gas exchange in humans. *Pflügers Arch* 441: 566–577, 2001.
9. Carson ER, Cobelli C, and Finkelstein, L. The mathematical modelling of metabolic and endocrine systems. New York: Wiley, p. 179–216, 1983.
10. Cautero M, Beltrami AP, di Prampero PE, and Capelli C. Breath-by-breath alveolar oxygen transfer at the onset of step exercise in humans. *Eur J Appl Physiol* 88: 203–213, 2002.
11. Cerretelli P, Pendergast DR, Paganelli WC, and Rennie DW. Effects of specific muscle training on the  $VO_2$  on-response and early blood lactate. *J Appl Physiol* 47: 761–769, 1979.
12. Cummin, AR, Iyawe VI, Mehta N, and Saunders KB. Ventilation and cardiac output during the onset of exercise, and during voluntary hyper-ventilation, in humans. *J Physiol* 370: 567–583, 1986.

13. **Daniel WW.** *Biostatistics: A Foundation for Analysis in the Health Science.* New York: Wiley, p. 602–605, 1991.
14. **De Cort SC, Innes JA, Barstow TJ, and Guz A.** Cardiac output, oxygen consumption and arterio-venous oxygen difference following a sudden rise in exercise level in humans. *J Physiol* 441: 501–512, 1991.
15. **di Prampero PE.** Energetics of muscular exercise. *Rev Physiol Biochem Pharmacol* 89: 143–222, 1981.
16. **di Prampero PE and Ferretti G.** The energetics of anaerobic lactic metabolism: a reappraisal of older and recent concepts. *Respir Physiol* 118: 103–115, 1999.
17. **di Prampero PE, Francescato MP, and Cettolo, V.** Energetics of muscle exercise at work onset: the steady-state approach. *Pflügers Arch* 445: 741–746, 2003.
18. **di Prampero PE and Lafortuna C.** Breath-by-breath estimate of alveolar gas transfer variability in man at rest and during exercise. *J Physiol* 415: 459–475, 1989.
19. **di Prampero PE and Margaria R.** Relationship between  $O_2$  consumption, high-energy phosphates, and the kinetics of the  $O_2$  debt in exercise. *Pflügers Arch* 304: 11–19, 1968.
20. **Elstad M, Toska K, and Walloe L.** Model simulations of cardiovascular changes at the onset of moderate exercise in humans. *J Physiol* 543: 719–728, 2002.
21. **Eriksen, M, Waaler BA, Walloe L, and Wesche J.** Dynamics and dimensions of cardiac output changes in humans at the onset and the end of moderate rhythmic exercise. *J Physiol* 426: 423–437, 1990.
22. **Fagraeus L and Linnarsson D.** Autonomic origin of heart rate fluctuations at the onset of muscular exercise. *J Appl Physiol* 40: 679–682, 1976.
23. **Ferretti, G, Binzoni T, Hulo N, Kayser B, Thomet JM, and Cerretelli P.** Kinetics of oxygen consumption during maximal exercise at different muscle temperatures. *Respir Physiol* 102: 261–268, 1995.
24. **Gallagher, KM, Fadel PJ, Strømstad M, Ide K, Smith SA, Querry RG, Raven PB, and Secher NH.** Effects of partial neuromuscular blockade on carotid baroreflex function during exercise in humans. *J Physiol* 533: 861–870, 2001.
25. **Gizdulich P, Prentza A, and Wesseling KH.** Models of brachial to finger pulse wave distortion and pressure decrement. *Cardiovasc Res* 33: 698–705, 1997.
26. **Grassi B, Gladden LB, Samaja M, Sary CM, and Hogan MC.** Faster adjustment of  $O_2$  delivery does not affect  $\dot{V}O_{2\text{-on}}$  kinetics in isolated in situ canine muscle. *J Appl Physiol* 85: 1394–1403, 1998.
27. **Grassi, B, Poole DC, Richardson RS, Knight DR, Erickson BK, and Wagner PD.** Muscle  $O_2$  uptake kinetics in humans: implications for metabolic control. *J Appl Physiol* 80: 988–996, 1996.
28. **Grönlund L.** A new method for breath-to-breath determination of oxygen flux across the alveolar membrane. *Eur J Appl Physiol* 52: 167–172, 1984.
29. **Iellamo F, Legramante JF, Raimondi G, and Peruzzi G.** Baroreflex control of sinus node during dynamic exercise in humans: effects of central command and muscle reflexes. *Am J Physiol Heart Circ Physiol* 272: H1157–H1164, 1997.
30. **Lamarra N, Whipp BJ, Ward SA, and Wasserman K.** Effect of interbreath fluctuations on characterising exercise gas exchange kinetics. *J Appl Physiol* 62: 2003–2012, 1987.
31. **Langewouters GJ, Wesseling KH, and Goedhard WJA.** The static elastic properties of 45 human thoracic and 20 abdominal aortas in vitro and the parameters of a new model. *J Biomech* 17: 425–435, 1984.
32. **Laughlin MH, Korthuis RJ, Duncker DJ, and Bashe RJ.** Control of blood flow to cardiac and skeletal muscle during exercise. In: *Handbook of Physiology. Exercise: Regulation and Integration of Multiple Systems.* Bethesda, MD: Am. Physiol. Soc., 1996, sect. 12, chapt. 16, p. 705–769.
33. **Linnarsson D.** Dynamics of pulmonary gas exchange and heart rate changes at start and end of exercise. *Acta Physiol Scand Suppl* 415: 1–78, 1974.
34. **Loeppky JA, Greene ER, Hoekenga DE, Caprihan A., and Luft UC.** Beat-by-beat stroke volume assessment by pulsed Doppler in upright and supine exercise. *J Appl Physiol* 50: 1173–1182, 1981.
35. **Mahler M.** First-order kinetics of muscle oxygen consumption, and an equivalent proportionality between  $QO_2$  and phosphorylcreatine level. Implications for the control of respiration. *J Gen Physiol* 86: 135–165, 1985.
36. **Meyer M and Scheid P.** Solubility of acetylene in human blood determined by mass spectrometry. *J Appl Physiol* 48: 1035–1037, 1980.
37. **Meyer RA.** A linear model of muscle respiration explains monoexponential phosphocreatine changes. *Am J Physiol Cell Physiol* 254: C548–C553, 1988.
38. **Miyamoto Y and Niizeki V.** Dynamics of ventilation, circulation, and gas exchange to incremental and decremental ramp exercise. *J Appl Physiol* 72: 2244–2254, 1992.
39. **Norton KH, Boushel R, Strange S, Saltin B, and Raven, PB.** Resetting of the carotid arterial baroreflex during dynamic exercise in humans. *J Appl Physiol* 87: 332–338, 1999.
40. **Ogoh, S, Fadel PJ, Nissen P, Jans O, Selmer C, Secher NH, and Raven PB.** Baroreflex-mediated changes in cardiac output and vascular conductance in response to alterations in carotid sinus pressure during exercise in humans. *J Physiol* 550: 317–324, 2003.
41. **Papelier Y, Escourrou P, Gauthier JP, and Rowell LB.** Carotid baroreflex control of blood pressure and heart rate in men during dynamic exercise. *J Appl Physiol* 77: 502–506, 1994.
42. **Potts JT and Mitchell JH.** Rapid resetting of carotid baroreceptor reflex by afferent input from skeletal muscle receptors. *Am J Physiol Heart Circ Physiol* 275: H2000–H2008, 1998.
43. **Potts JT, Shi XR, and Raven PB.** Carotid baroreflex responsiveness during dynamic exercise in humans. *Am J Physiol Heart Circ Physiol* 265: H1928–H1938, 1993.
44. **Rådegran G and Saltin B.** Muscle blood flow at onset of dynamic exercise in man. *Am J Physiol Heart Circ Physiol* 274: H314–H322, 1998.
45. **Rossiter HB, Ward SA, Doyle VL, Howe FA, Griffiths JA, and Whipp BJ.** Inferences from pulmonary  $O_2$  uptake with respect to intramuscular [phosphocreatine] kinetics during moderate exercise in humans. *J Physiol* 518: 921–932, 1999.
46. **Rossiter HB, Ward SA, Kowalchuk JM, Howe FA, Griffiths JR, and Whipp BJ.** Dynamic asymmetry of phosphocreatine concentration and  $O_2$  uptake between the on- and off-transients of moderate- and high-intensity exercise in humans. *J Physiol* 541: 991–1002, 2002.
47. **Rowell LB, O’Leary DS, and Kellogg DL Jr.** Integration of cardiovascular control systems in dynamic exercise. In: *Handbook of Physiology. Exercise: Regulation and Integration of Multiple Systems.* Bethesda, MD: Am. Physiol. Soc., 1996, sect. 12, chapt. 17, p. 770–838.
48. **Sheriff DD, Rowell LB, and Scher AM.** Is rapid rise in vascular conductance at onset of dynamic exercise due to muscle pump? *Am J Physiol Heart Circ Physiol* 265: H1227–H1234, 1993.
49. **Tam E, Azabji Kenfack M, Cautero M, Lador F, Antonutto G, di Prampero PE, Ferretti G, and Capelli C.** Correction of cardiac output obtained by Modelflow from finger pulse pressure profiles with a respiratory method in humans. *Clin Sci* 106: 371–376, 2004.
50. **Toska K and Erickson M.** Peripheral vasoconstriction shortly after onset of moderate exercise in humans. *J Appl Physiol* 77: 1519–1525, 1994.
51. **van Lieshout JJ, Toska K, van Lieshout EJ, Eriksen, M, Walloe L, and Wesseling KH.** Beat-to-beat non-invasive stroke volume from arterial pressure and Doppler ultrasound. *Eur J Appl Physiol* 90: 131–137, 2003.
52. **Walloe L and Wesche J.** Time course and magnitude of blood flow changes in the human quadriceps muscle during and following rhythmic exercise. *J Physiol* 405: 257–273, 1988.
53. **Wasserman K, Whipp BJ, and Castagna J.** Cardiodynamic hyperpnea: hyperpnea secondary to cardiac output increase. *J Appl Physiol* 36: 457–464, 1974.
54. **Weissman C, Abraham B, Askanazi J, Milic-Emili J, Hyman AI, and Knney JM.** Effect of posture on the ventilatory response to  $CO_2$ . *J Appl Physiol* 53: 761–765, 1982.
55. **Wesseling KH, Jansen JRC, Settels JJ, and Schreuder JJ.** Computation of aortic flow from pressure in humans using a nonlinear, three-element model. *J Appl Physiol* 74: 2566–2573, 1993.
56. **Whipp BJ and Ward SA.** Physiological determinants of pulmonary gas exchange kinetics during exercise. *Med Sci Sports Exerc* 22: 62–71, 1990.
57. **Whipp BJ, Ward SA, Lamarra N, Davis, JA, and Wasserman, K.** Parameters of ventilatory and gas exchange dynamics during exercise. *J Appl Physiol* 52: 1506–1513, 1982.
58. **Whipp BJ and Wasserman K.** Effect of anaerobiosis on the kinetics of  $O_2$  uptake during exercise. *Fed Proc* 45: 2942–2947, 1986.
59. **Yoshida T and Whipp BJ.** Dynamic asymmetries of cardiac output transients in response to muscular exercise in man. *J Physiol* 480: 355–359, 1994.
60. **Yoshida T, Yamamoto K, and Udo M.** Relationship between cardiac output and oxygen uptake at the onset of exercise. *Eur J Appl Physiol* 66: 155–160, 1993.